

## Winding Trajectories for Dry Filament Wound Preforms

T. SOFI<sup>1</sup> and R. SCHLEDJEWSKI<sup>1,2</sup>

<sup>1</sup>Christian Doppler Laboratory for Highly Efficient Composite  
Processing, Montanuniversität Leoben, Otto Glöckel-Straße 2/I, 8700  
Leoben, Austria

Email: [tasdeeq.sofi@unileoben.ac.at](mailto:tasdeeq.sofi@unileoben.ac.at), Web Page: <http://www.kunststofftechnik.at/de/5540/>

<sup>2</sup>Processing of Composites Group, Department of Polymer Engineering  
and Science, Montanuniversität Leoben, Otto Glöckel-Straße 2/III, 8700  
Leoben, Austria

Email: [Ralf.Schledjewski@uinleoben.ac.at](mailto:Ralf.Schledjewski@uinleoben.ac.at), Web Page: <http://www.kunststofftechnik.at/de/5534/>

**Keywords:** Winding Angle; Friction Coefficient; Design Space; Geodesic; Non-geodesic

### Abstract

The aim of this study is to investigate the influence of friction coefficient and to a lesser the influence of initial winding angle on the winding angle development along a conical surface. Then to obtain the feasible design space for wet and dry winding and generate different winding trajectories on the conical mandrel surface. The equations for winding angle and coordinates of the fiber trajectory have been developed for a truncated cone using differential geometry. The influence of initial winding angle and friction coefficient on the distribution of winding angles along the height of the cone has been investigated. The feasible design space has been obtained for two different friction coefficients corresponding to wet and dry winding. Winding trajectories namely geodesic, non-geodesic and constant winding angle has been generated on the truncated cone. The results show that friction coefficient has a huge effect on the winding angle development and can significantly enlarge the design flexibility. It can be used to manipulate the fiber trajectories without causing slippage. A combined path can be achieved from a non-geodesic and a constant winding angle path to achieve a specific fiber direction. The combined path meets the necessary requirements in filament winding process and can be used to enhance the structural performance of the truncated cone by placing the fibers along the principal stress directions.

### 1. Introduction

Filament winding is one the main manufacturing processes in composite industry. It is a well-established process mostly used to manufacture surfaces of revolution. Three types of winding processes can be identified viz., wet winding, pre-preg and dry winding. The principle difference in dry winding as compared to the other two types of winding processes is that in dry winding the impregnation of the fiber material is carried after the winding process. The other major difference between dry and wet winding is that during

the processing of dry winding, the friction coefficient can exceed 0.5. Whereas, the friction coefficient generated during wet winding is around 0.2 [1].

In filament winding two types of trajectories namely, geodesic and non-geodesic are generally implemented to wind fibers on a mandrel surface. Geodesic paths are defined as the shortest paths between any two arbitrary points on a surface. Geodesic paths are stable and do not require any external force to keep them from slipping off the mandrel surface. However, to enlarge the design flexibility paths known as non-geodesic are used. These paths are not stable and require frictional forces to keep them from slipping off the mandrel surface. This makes friction coefficient one the most important factor in filament winding which controls the scope of the winding trajectories. The other important parameter which affects the winding trajectory is the initial winding angle.

The aim of this paper is to discuss how friction coefficient and initial winding angle affects the winding angle distribution over the surface of a truncated cone and to study the different types of winding trajectories feasible on the cone. First, the mathematical equations have been formed. Then the influence of friction coefficient and initial winding angle on the development of winding angle along the height of the cone has been investigated. In section (2.3), the slippage factor has been obtained with respect to winding angle and geodesic curvature in order to obtain the feasible design space for wet and dry winding. Then the winding trajectories including geodesic, non-geodesic, constant winding angle and a combination of these trajectories have been generated for a conical shape.

### Mathematical formulation

A general surface of revolution in a polar coordinate system with parameters  $(u, v)$  is represented as:

$$S(u, v) = \{f(v) \cos(u), f(v) \sin(u), g(v)\} \quad (1)$$

As mentioned before while winding fibers along a non-geodetic path, the fiber experiences slippage. The generated frictional forces must be enough to keep the fibers from slipping off the mandrel surface. The condition for the fiber to be stable on the surface is given by [2, 3]:

$$\mu \geq \lambda = \left| \frac{k_g}{k_n} \right| \quad (2)$$

Where  $\mu$  is the coefficient of friction generated between the fiber and the mandrel surface or between the fiber and previously wound fiber layer.  $\lambda$  denotes the slippage tendency.  $k_g$  and  $k_n$  are the geodesic and normal curvature at any point belonging to the fiber path respectively. The equations for geodesic and normal curvature for a general surface of revolution are given by [4]:

$$k_g = -\frac{d\alpha \cos\alpha}{dv \sqrt{G}} - \frac{1}{2} \frac{E'(v) \sin\alpha}{E \sqrt{G}} \quad (3)$$

$$k_n = k_1 \cos^2 \alpha + k_2 \sin^2 \alpha \quad (4)$$

Where  $E = S'(u) \cdot S'(u)$ ,  $F = S'(u) \cdot S'(v)$  and  $G = S'(v) \cdot S'(v)$  are the coefficients of first fundamental form.  $k_1$  and  $k_2$  are the principal curvatures along meridional and parallel directions and  $\alpha$  is called the winding angle.

Using these in Eq. (2), the equation for fiber path is [4]:

$$\frac{d\alpha}{dv} = -\frac{1}{2} \frac{E'(v)}{E} \tan \alpha \pm \frac{\mu \sqrt{G}}{\cos \alpha} [ (k_1 \sin^2 \alpha + k_2 \cos^2 \alpha) ] \quad (5)$$

For a conical surface  $f(v) = r$ ,  $u = \phi$  and  $g(v) = z(r)$  i.e.

$$S(r, \phi) = \{r \cos(\phi), r \sin(\phi), z(r)\} \quad (6)$$

Where  $(r, \phi, z)$  represents the radial, angular and axial coordinates respectively. The generatrix function  $z(r)$  for a truncated cone with a pole radius of  $r_1$ , equatorial radius of  $r_2$  and half-apex angle  $\theta$  is given by:

$$z(r) = (r_2 - r) \cot \theta \quad (7)$$

The coefficients of the first fundamental form are:

$$E = r^2, F = 0 \text{ and } G = 1 + z'(r)^2 \quad (8)$$

The geodesic and normal curvature and the equation describing the fiber path are calculated as follows:

$$k_g = -\frac{d\alpha}{dr} \frac{\cos \alpha}{\operatorname{cosec} \theta} - \frac{\sin \theta \sin \alpha}{r}; \quad k_n = \frac{1}{r \sec \theta} \sin^2 \alpha \quad (9)$$

$$\frac{d\alpha}{dr} = \frac{-\mu \sin^2 \alpha \cot \theta - \sin \alpha}{r \cos \alpha} \quad \text{or} \quad \frac{d\alpha}{dz} = \frac{\mu \sin^2 \alpha + \sin \alpha \tan \theta}{(r_2 - z) \tan \theta \cos \alpha} \quad (10)$$

For  $\mu = 0$  and after integration, this equation reduces to Clairaut relation. Which describes a geodesic path on a surface. The Clairaut relation for a conical surface with a pole radius of  $r_1$  is [4]:

$$r = \frac{r_1}{\sin \alpha} \quad (11)$$

The solution of Eq. (10) with the boundary condition that alpha =  $\pi/2$  radians at the pole is given by [5]:

$$\alpha = \sin^{-1} \left[ \frac{r_1}{\mu(r - r_1) \cot \theta + r} \right] \quad (12)$$

Stability condition to avoid slippage is given by:

$$\mu \geq \lambda = \left| \frac{-\frac{d\alpha}{dr} \cos \alpha - \frac{\sin \theta \sin \alpha}{r}}{\frac{1}{r \sec \theta} \sin^2 \alpha} \right| \quad (13)$$

The coordinates of the fiber trajectory can be calculated as follows [5]:

$$\phi(r) = \int_{r_1}^{r_2} \sqrt{\frac{G}{E}} \tan(\alpha) dr \quad (14)$$

To obtain the fiber trajectory Eq. (10) is solved for  $\alpha$  and then used in Eq. (14) to obtain the coordinates of the fiber path.

## 2. Results and discussion

The results have been obtained for a cone with  $r_1 = 150$  mm,  $r_2 = 750$  mm, half-apex angle =  $30^\circ$ .

### 2.1. Influence of initial winding angle and friction coefficient on winding angle development

The influence of initial winding angle prescribed at the equator ( $Z = 0$ ) and friction coefficient on the development of winding angle along the height of the cone has been obtained by solving Eq. (10) using fourth order Runge-Kutta method [6]. In Fig. 1, the winding angle distribution has been plotted for different initial winding angles keeping friction coefficient constant ( $\mu = 0.1$ ). Fig. 2 describes the winding angle development for different friction coefficients at a constant initial winding angle of  $7^\circ$ . It is observed that increasing the friction coefficient as well as initial winding angle leads to an overall increase in the winding angle distribution, as the path is traced from equator to pole. For e.g. for a friction coefficient of 0.45, the winding angle distribution can be obtained from  $7^\circ$  to  $78.87^\circ$  as compared to  $7^\circ$  to  $47.08^\circ$  for a friction coefficient of 0.2. These parameters have a large effect on the winding angle distribution and can be used to manipulate the fiber path. One of the important point to observe is that beyond a certain friction coefficient (0.45) and initial winding angle ( $10^\circ$ ), the fiber cannot reach the pole area of the cone. This shows that the fiber path and therefore the design space is restricted by friction coefficient and the initial winding angle.

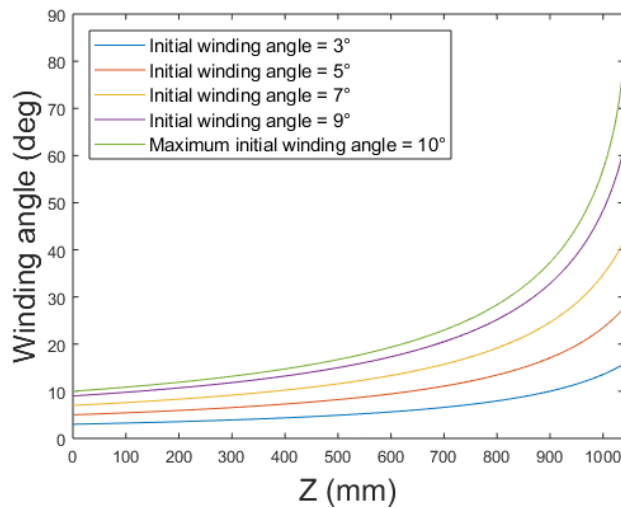


Fig. 1: Influence of initial winding angle on the winding angle distribution along the conical surface.

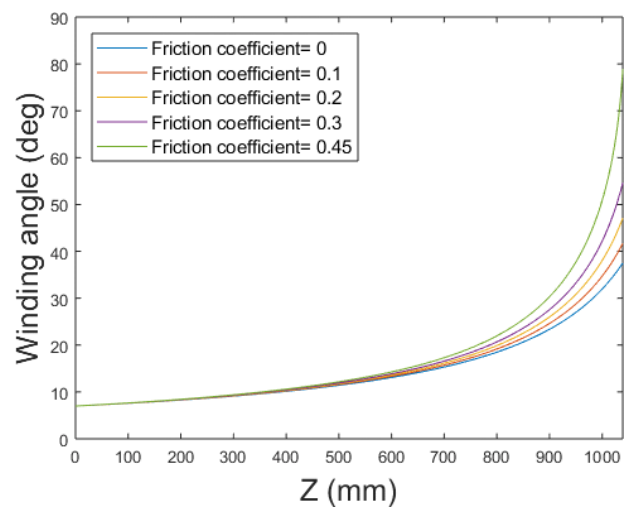


Fig. 2: Influence of friction coefficient on the winding angle distribution along the conical surface.

## 2.2. Influence of friction coefficient and Geodesic curvature ( $k_g$ ) on design space

The fiber trajectories on a mandrel surface in filament winding are primarily restricted by the availability of friction coefficient. As the geodesic curvature increases, the fiber trajectories move away from a geodesic path. This requires higher friction coefficients to keep the fiber stable on the mandrel surface. Using Eq. (13), two graphs (Fig. 3 and Fig. 4) have been plotted for friction coefficients of 0.2 and 0.5 corresponding to wet and dry winding respectively. Both plots show an exponential increase of slippage tendency as a function of increasing geodesic curvature and decreasing winding angles. The line corresponding to zero geodesic curvature is a geodesic path. For such a path the fibers can be wound at any winding angle from  $0^\circ$  to  $90^\circ$ , without the requirement of the frictional forces. For non-zero geodesic curvature space, the feasibility of the winding paths depends upon the availability of the frictional forces. The feasible design space for the two friction coefficients is shown by magenta dotted region. As observed from these plots friction coefficient significantly enlarges the design space. Therefore, higher friction coefficients can allow winding trajectories further away from geodesic paths. Since higher friction coefficients can be achieved for dry winding as compared to wet winding. Therefore, the winding trajectories for dry winding have a larger scope than those that can be achieved in the wet winding.

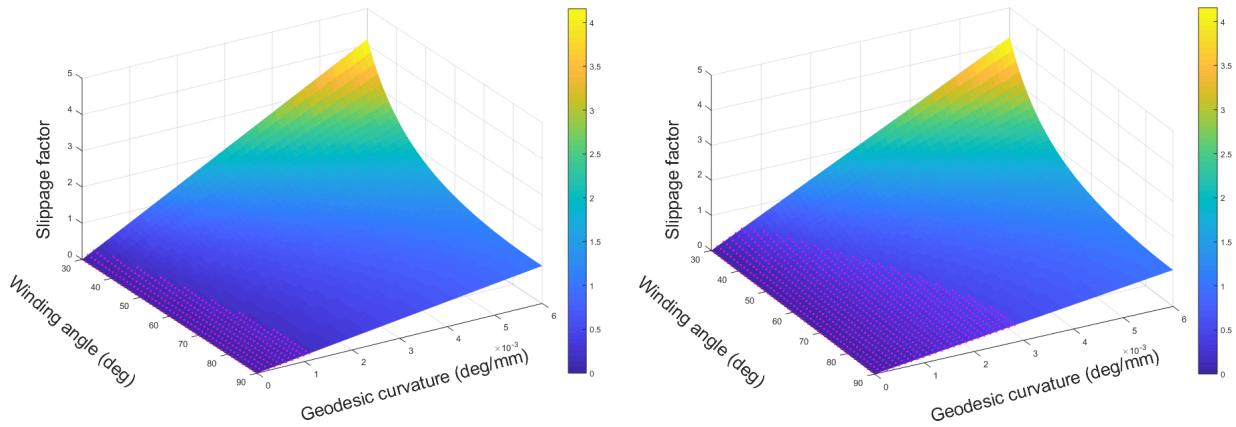


Fig. 3 and Fig. 4: Feasible design space for a friction coefficient of 0.2 (wet winding) and 0.5 (dry winding).

## 2.3. Winding trajectories

### Geodesic and non-geodesic paths

The geodesic and non-geodesic paths are obtained by solving Eq. (10) with a boundary condition that winding angle at the polar region is  $\pi/2$  radians, which is important for the continuation of the fiber path in filament winding. Then the fiber path coordinates are obtained from Eq. (14). A geodesic path is generated by setting  $\mu = 0$ . The geodesic path on the cone is shown by the magenta curve in Fig. 5.

The other paths (blue) correspond to non-geodesic paths with  $\mu$  ranging from 0.1 – 0.5 from left to right as shown in the Fig. 5. These paths deviate from geodesic paths by a smaller extent and are generally feasible in filament winding. As can be observed by making the use of the frictional forces a deviation from the geodesic paths is possible. This leads to an increase in the design flexibility and allows for broader distribution of winding angles over the surface of the cone without causing slippage. Therefore, the friction coefficient is the most important parameter which decides the extent and stability of the winding trajectories in filament winding.

### Constant winding angle path

An alternative path that is possible is a constant winding angle path. The constant winding angle path is required to meet specific fiber directions. This is important while optimizing the paths along the principal stress directions. In Fig. 6, constant winding angle paths have been generated for  $45^\circ$ ,  $42.5^\circ$  and  $40^\circ$  from left to right. However, in filament winding it is necessary that winding angle at the polar regions must be  $\pi/2$  radians to ensure a continuation of the fiber path. Therefore, a path obtained by combining a non-geodesic and a constant winding angle path can be generated. This path satisfies the requirements for path continuation and allows the fiber to follow a certain path at least on most part of the mandrel surface.

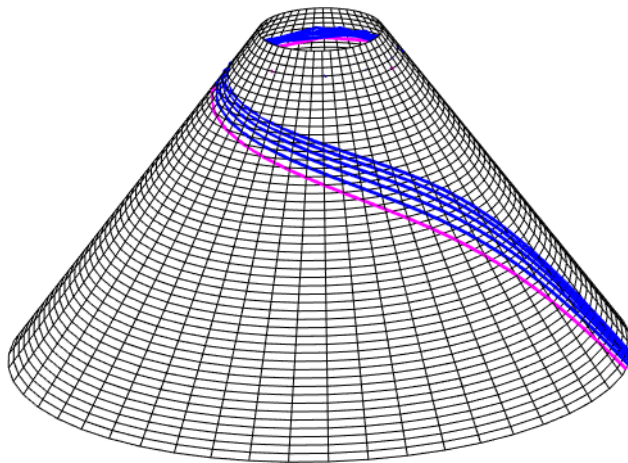


Fig. 5: Geodesic and non-geodesic trajectories on the truncated cone.

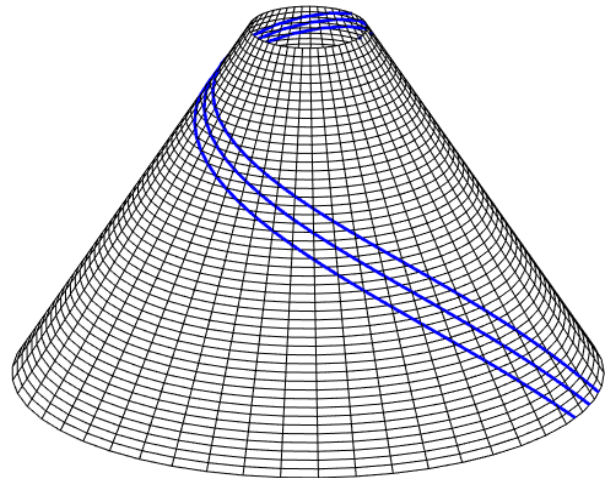


Fig. 6: Constant winding angle trajectories on the truncated cone.

### Combined path

Two combined winding paths have been generated. The winding angle development is shown in Fig. 7 and Fig. 8. Path 1 is generated with a constant winding angle of 45° and connected with a non-geodesic path which has been generated with a friction coefficient of 0.155. The angle at the connecting point should be same (45°) and the winding angle at the pole is  $\pi/2$  radians. Similarly, path 2 has been generated by connecting a constant winding angle path of 42.5° with a non-geodesic path generated by using a friction coefficient of 0.1. In this way, a stroke can be generated and continuation of the fiber path can be ensured in the polar region. Thus, necessary requirements for filament winding process can be met.

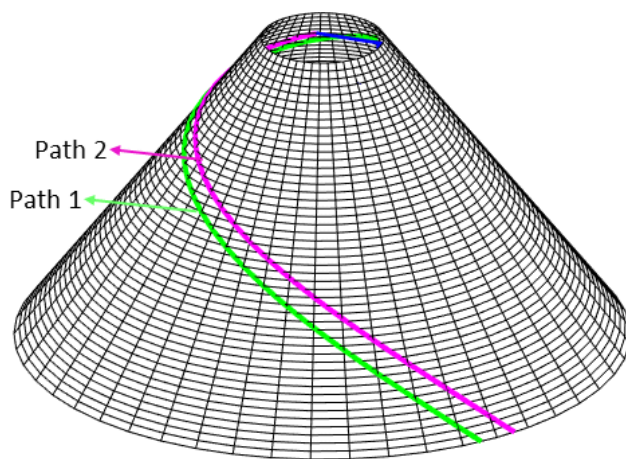


Fig. 7: Combined path for a non-geodesic and a constant winding angle path.

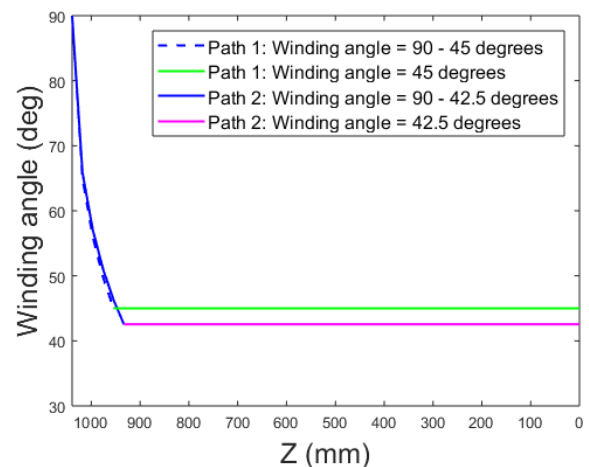


Fig. 8: Variation of winding angle for a combined path.

### 3. Conclusion

The influence of friction coefficient and initial winding angle on the winding angle development for geodesic and non-geodesic trajectories on a conical surface was investigated. It was observed that both of these parameters increase the distribution of winding angles over the surface of the cone. The slippage tendency was plotted with respect to geodesic curvature and winding angles. The feasible design space was obtained for two different friction coefficients corresponding to wet and dry winding. It was shown how friction coefficient can significantly enlarge the design space. Winding trajectories for a single stroke were generated on the conical surface for geodesic, non-geodesic and constant winding angle paths. In the end, it was shown how a non-geodesic and a constant winding angle path can be connected to generate a combined path that meets the requirements necessary for the filament winding process.

### Acknowledgement

The financial support by the Austrian Federal Ministry for DIGITAL and ECONOMIC AFFAIRS is gratefully acknowledged. Furthermore, the financial support of the Christian Doppler Laboratory for Highly Efficient Composite Processing by the FACC Operations GmbH is kindly acknowledged.

### References

- [1] V.V. Vasiliev, A.A. Krikanov, and A.F. Razin. New generation of filament-wound composite pressure vessels for commercial applications, *Composite Structures*, 62: 449–459, 2003.
- [2] L. ZU, S. Koussios, and A. Beukers. Design of filament-wound domes based on continuum theory and non-geodesic roving trajectories, *Composites Part A: Applied Science and Manufacturing*, 41: 1312–1320, 2010.
- [3] R. Wang, W. Jiao, W. Liu, F. Yang, and X. He. Slippage coefficient measurement for non-geodesic filament-winding process, *Composites Part A: Applied Science and Manufacturing*, 42: 303–309, 2011.
- [4] S. Koussios, O.K. Bergsma, and G. Mitchell. Non-geodesic filament winding on generic shells of revolution, *Proceedings of the Institution of Mechanical Engineers, Part L: Journal of Materials: Design and Applications*, 219: 25–35, 2005.
- [5] Sotiris Koussios. *Filament Winding: A Unified Approach*. Dissertation an der Tu Delft, 2004.
- [6] Lei Zu, Qinxiang He, Junping Shi, Hui Li, Ed. *Non-Geodesic Trajectories for Filament Wound Composite Truncated Conical Domes*. Trans Tech Publications, Switzerland, 2012.